CEAS EuroGNC 2019
"Conference on Guidance, Navigation and Control"
3-5 April 2019 @ Politecnico di Milano, Milan, Italy.

CEAS-GNC-2019-042

Air-to-air automatic landing for multirotor UAVs

P. Giuri, A. Marini Cossetti, M. Giurato, D. Invernizzi and M. Lovera

Abstract Nowadays, Unmanned Aerial Vehicles (UAVs) are continuing to enlarge their market share and the related research activities are growing exponentially. In particular, the interaction between two or more vehicles during flight (*e.g.*, formation flight and refuelling) are getting more and more attention. When dealing with intelligence, surveillance, and reconnaissance missions, the problem of air-to-air refuelling can arise when undertaking long range flights. In the military field, Air-to-Air Automatic Refuelling (AAAR) involving fixed-wing drones is object of studies and research activities. Also small UAVs suffer from low endurance problems, since the overwhelming majority of them has an electric propulsion system. A possibility to extend the range of UAV missions could be to have a carrier drone, reasonably a fixed-wing one, with several lightweight multirotors aboard, which can take-off from and land on it. The work conducted within this project is focused on the implementation of two nonlinear time-optimal guidance laws to obtain an air-to-air automatic landing of a small quadcopter on a bigger octocopter as a carrier. Eventually, the proposed guidance laws are validated through experimental activities.

1 Introduction

An Unmanned Aerial Vehicle (UAV) is an aircraft without a pilot aboard, which is able to fly autonomously or could be piloted remotely from the ground. Usually called *drones*, in recent years these vehicles has met great interest both in civil and military fields thanks to their wide range of applications, including precision agriculture, photography, patrolling and surveillance, search and rescue, entertainment, product delivery, aerial inspection and many others. When referring to drones, one usually refers to the category of multi-rotor Vertical Take-Off and Landing (VTOL)

P. Giuri, A. Marini Cossetti, M. Giurato, D. Invernizzi, M. Lovera,
Dipartimento di Scienze e Tecnologie Aerospaziali, Politecnico di Milano e-mail: {pietro.giuri, adriano.marini}@mail.polimi.it, {mattia.giurato, davide.invernizzi, marco.lovera}@polimi.it

vehicles of small/medium size provided with a number of rotors greater than two and remotely controlled. Their versatility in technical operations has pushed the commercial and research communities towards new challenges. New research activities involve the possibility to remotely command many drones simultaneously, following a given path or performing a task in a cooperative way and autonomously, see [1, 2, 3]. Among the main sub-areas covering the cooperative control problem of UAVs, formation flight has attracted great interest and has been widely investigated. Besides multi-rotors formation flight, in the literature it is possible to find researches related to the Air-to-Air Automatic Refuelling (AAAR) involving fixed-wing drones (see [4, 5, 6]). Furthermore, also the landing of a multirotor on a moving platform is a consolidated problem (see [7, 8, 9]) as well as the landing on a tilted platform (see [10]) or a vertically oscillating one (see [11]) but none of them involves a flying platform. In this paper we present the results obtained thanks to the design and implementation of two guidance laws aimed at providing to a small multirotor a time-optimal reference descent trajectory, ending up to an air-to-air automatic landing on a larger multirotor in hovering conditions. This kind of manoeuvre is risky because the propellers wake of a multirotor generates an unsteady flow field around it, and when two UAVs fly in close proximity, they perturb each other. For what regards the air-to-air landing operation, one drone is always above the other which constantly flies in a perturbed regime. The closer the vehicles, the stronger will be the aerodynamic disturbances affecting the one below. It is straightforward that the aerodynamic forces developing on the multirotors may vary continuously in this flight condition. Other obvious considerations may be done regarding the dimensions and weights of the UAVs, *i.e.*, the carrier drone must be heavier and larger than the landing one, in order to stand its weight once the touch-down occurs. A simple way of realising the landing manoeuvre without involving any centralisation of the landing control system consists in generating a suitable guidance law for the follower/lander while keeping the carrier at a fixed altitude (possibly fixed position). In this framework, the landing can be realised using the standard on-board attitude and position controllers and simply adding to the lander control system suitable guidance law generation functions.

In view of the above discussion, the aim of this paper is to demonstrate the feasibility of air-to-air landing of multirotor UAVs and to compare the performance achieved using two different time-optimal guidance laws. For the sake of simplicity, the problem of a pure vertical landing manoeuvre is studied, i.e., perfect in-plane synchronisation of the motion of the UAVs is assumed.

The paper is organised as follows: Section 2 described the control architecture of the considered multirotors, while in Section 3 the studied guidance laws are presented. Section 4 deals with the digital implementation of the guidance laws, Section 5 describes the implemented safety checks while Section 6 and Section 7 present respectively the experimental set-up and the obtained results.

2 UAVs control architecture

The typical control architecture of a multirotor UAV is defined with nested control loops, as can be seen in Figure 1. Usually such configuration has an outer position control loop which generates the thrust set-point ($f_c = [0,0,-T^o]^T$) and the attitude set-point (q^o) for the inner attitude control loop. In particular, such position control loop is based on an inner PID loop for the linear velocity and an outer P loop for the position itself. The attitude controller instead generates the required moments set-point (τ_c) to achieve the attitude tracking. As well, such controller is based on an inner PID loop for the angular velocity and an outer P loop for the angular position. Finally a control allocator (*i.e.*, the *Mixer* block) is defined according to the multirotor frame/configuration in order to convert the force/moments set-points into propeller angular velocity commands (Ω_i). The UAV Navigation module, which is integrated in the Flight Control Unit (FCU), provides then the state estimates ($\hat{p},\hat{v},\hat{q},\hat{\omega}$) which will be used as a feedback for the control loops described above.

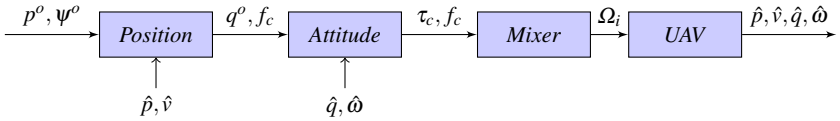

Fig. 1 Flight control architecture

Due to the described control configuration, any guidance law has to consider the position ($p^o = [N^o, E^o, D^o]^T$) and the heading (ψ^o) set-points as control variables.

For the purpose of this project, the heading dynamics and the horizontal plane synchronization are assumed to be perfect and only the vertical (landing) path generation will be considered.

3 Nonlinear time-optimal guidance laws

The landing objective may be described as:

$$\lim_{t \to t_l} z_r(t) = D_t(t) - D_f(t) = 0, \tag{1}$$

where the subscripts f and t will be used to describe any quantity of the landing drone (*follower*) and of the carrier drone (*target*) respectively, t_l is the landing time and z_r is the relative position.

Clearly, the landing procedure is subject to physical constraints. The first one is on the *Down* component of position:

$$D_f(t) \leq D_t(t) \Rightarrow z_r(t) \geq 0, \quad t > t_0, \tag{2}$$

where t_0 is the starting time of the landing manoeuvre. This means that the follower must be always above the target from starting time onward. In addition, the relative velocity ($\dot{z}_r$) between the vehicles must be as small as possible at final time, *i.e.*:

$$\lim_{t \to t_l} \dot{z}_r(t) = \dot{D}_t(t) - \dot{D}_f(t) = 0. \tag{3}$$

Additionally, it has been decided to impose this problem to be time-optimal:

$$\min J = \int_{t_0}^{t_l} dt = t_l - t_0, \tag{4}$$

and the UAV-follower acceleration $\ddot{D}_f$ to be bounded during the landing procedure

$$\ddot{D}_f \in [\ddot{D}_f^{dec}, \ddot{D}_f^{acc}], \tag{5}$$

where $\ddot{D}_f^{dec} < 0$ is the maximum upward deceleration and $\ddot{D}_f^{acc} > 0$ is the maximum downward acceleration.

Since the target UAV is assumed to hover, the follower vertical acceleration is certainly greater than the target one, then:

$$\ddot{z}_r = \ddot{D}_t - \ddot{D}_f \approx -\ddot{D}_f, \tag{6}$$

which means the follower acceleration bounds may be applied directly to the relative acceleration.

3.1 Bang-bang control

To solve a time-optimal path generation with saturations in the acceleration set-point it is well known that a *bang-bang* control logic is the optimal solution (see [12]), where the control variable is the relative acceleration:

$$u(t) = \ddot{z}_r^o(t). \tag{7}$$

The relative landing path is then obtained by integration:

$$\dot{z}_r^o(t) = \int_{t_0}^{t_l} u(t)dt + \dot{z}_r(t_0), \tag{8}$$

$$z_r^o(t) = \int_{t_0}^{t_l} \dot{z}_r^o(t)dt + z_r(t_0), \tag{9}$$

while the absolute landing path will be:

$$D_f^o(t) = D_t(t) - z_r^o(t). \tag{10}$$

It is proved that the optimal control $u^*(t)$ may be defined as follows:

$$u^*(t) = \begin{cases} -\ddot{D}_f^{dec} & \text{if} \quad [\dot{z}_r(t)]^2 sign(\dot{z}_r(t)) \leq -2z_r(t), \\ -\ddot{D}_f^{acc} & \text{if} \quad [\dot{z}_r(t)]^2 sign(\dot{z}_r(t)) > -2z_r(t), \end{cases} \tag{11}$$

where the $sign(x)$ function is defined as follows:

$$sign(x) = \begin{cases} +1 & \text{if} \quad x \geq 0, \\ -1 & \text{if} \quad x < 0. \end{cases} \tag{12}$$

Such control law will produce a linearly increasing desired velocity with a consequently parabolic position trajectory and for a high initial relative distance the required velocity might reach undesired high speeds.

3.2 Bang-zero-bang control

A possible solution to keep the required velocity bounded is to impose in the optimisation problem the following additional constraint:

$$|\dot{z}_r^o| \leq \dot{D}_{max}^o, \tag{13}$$

which will results in a *bang-zero-bang* control law. A similar approach has been presented in [11] where the follower UAV had to land on an oscillating platform.

The optimal control $u^*(t)$ may be then defined as follows:

$$u^*(t) = \begin{cases} -\ddot{D}_f^{dec} & \text{if} \quad \hat{z}_r(t+\Delta t) < 0, \\ 0 & \text{if} \quad \hat{z}_r(t+\Delta t) \geq 0 \wedge |\dot{z}_r^o(t)| \geq \dot{D}_{max}^o, \\ -\ddot{D}_f^{acc} & \text{if} \quad \hat{z}_r(t+\Delta t) \geq 0, \end{cases} \tag{14}$$

where $\hat{z}_r(t+\Delta t)$ is an estimate of the relative position after at time $t+\Delta t$. Δt can be computed as the time needed to reach the relative velocity $\dot{z}_r(t+\Delta t) = 0$ given the actual relative velocity and maximum upward deceleration achievable $-\ddot{D}_f{}^{dec}$ and it can be formulated as:

$$\Delta t = -\frac{\dot{z}_r(t)}{\ddot{D}_f^{dec}}, \tag{15}$$

$$\hat{z}_r(t+\Delta t) = z_r(t) + \dot{z}_r(t)\Delta t - \frac{1}{2}\ddot{D}_f^{dec}\Delta t^2. \tag{16}$$

As well as the *bang-bang* case, the position trajectory is calculated as described in equations (8) to (10).

4 Digital implementation

The algorithms presented in the previous section have been implemented digitally in MATLAB since the guidance law which controls the trajectories of both UAVs will be executed online using a MATLAB script as will better explained in the following section.

The main difference between the described algorithm and the digital implementation is about the numerical integration of the velocity and position set-point obtained starting from the acceleration command, which is carried out as follows:

$$\dot{z}_r^o(k) = u(k)dt + \dot{z}_r^o(k-1), \tag{17}$$
$$z_r^o(k) = \dot{z}_r^o(k)dt + z_r^o(k-1), \tag{18}$$
$$D_f^o(k) = D_t^o(k) - z_r^o(k), \tag{19}$$

where dt is the integration time and the initial conditions are given by the measured relative velocity and positions at the beginning of the landing manoeuvre t_0:

$$\dot{z}_r^o(0) = \dot{z}_r(t_0), \tag{20}$$
$$z_r^o(0) = z_r(t_0). \tag{21}$$

During the execution of the landing manoeuvre, the target UAV is assumed to fly in hover, then the altitude set-point is kept constant:

$$D_t^o(k) = D_t^o \quad \forall k \geq 1 \tag{22}$$

5 In-plane synchronization and safety checks

As has been mentioned in Section 2, heading and in-plane dynamics are neglected since the target UAV is assumed to be in hover condition and its *North* and *East* set-points are kept constant:

$$N_t^o(k) = N_t^o \quad \forall k \geq 1, \tag{23}$$
$$E_t^o(k) = E_t^o \quad \forall k \geq 1. \tag{24}$$

Concerning the follower, during the execution of the landing the horizontal set-points will be the measurements of the horizontal position of the target:

$$N_f^o(k) = N_t(k) \quad \forall k \geq 1, \tag{25}$$
$$E_f^o(k) = E_t(k) \quad \forall k \geq 1. \tag{26}$$

To increase the safety of the landing execution, at every iteration step the horizontal relative position between the target and the follower (H_{tf}) is checked to be within a given bound ($H_b(z_r)$) which depends linearly on the vertical relative posi-

tion in order to obtain a *cone-shaped* safety volume:

$$H_{tf}(k) = \sqrt{(N_t(k) - N_f(k))^2 + (E_t(k) - E_f(k))^2}, \tag{27}$$

$$H_b(z_r(k)) = mz_r(k) + q, \tag{28}$$

$$if \quad H_{tf}(k) < H_b(z_r(k)) \implies \text{safe}, \tag{29}$$

with m and q suitably chosen coefficients.

If the constraint is not satisfied the landing manoeuvre is stopped and the vertical relative distance is hold until the horizontal relative distance is within the bound again.

In Figure 2 it is possible to evaluate the horizontal relative position and the safety cone over time obtained during a flight test.

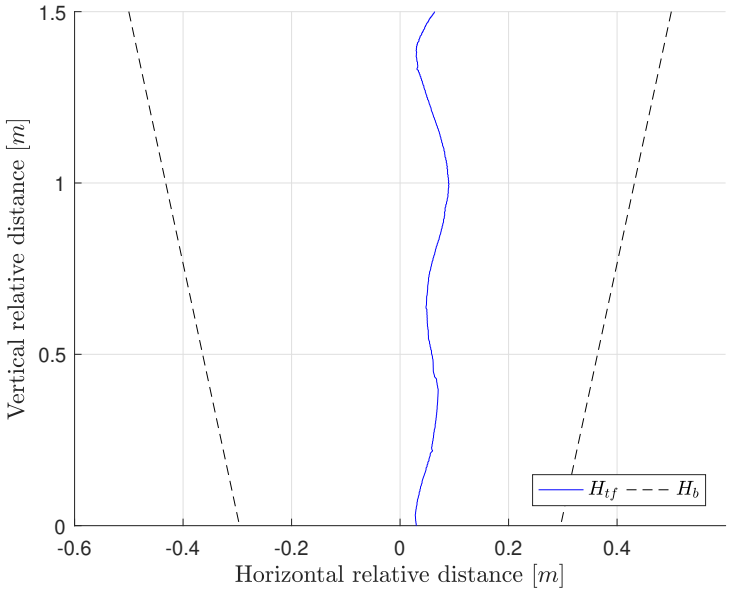

Fig. 2 Horizontal distance between the follower and the target

6 Experimental set-up

The landing algorithms have been tested using the multirotor platforms shown in Figure 3 inside the Flying Arena for Rotorcraft Technologies (FlyART) of Politecnico di Milano (see Figure 4) which is an indoor facility equipped with a motion capture system (Optitrack) and a flight volume of $6 \times 12 \times 4$ m.

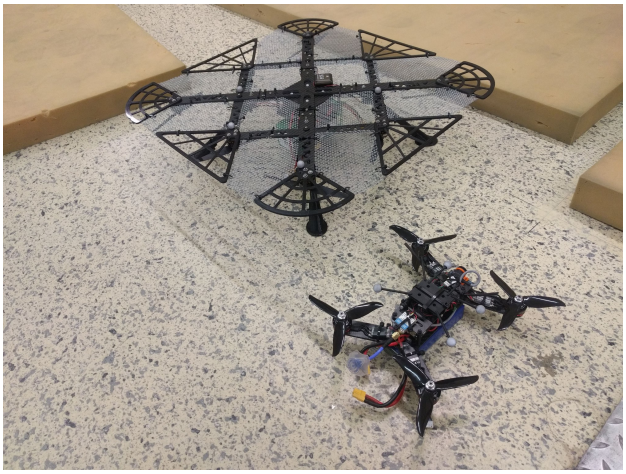

Fig. 3 The CARRIER-1 and ANT-R multirotor UAVs used in the experimental activities

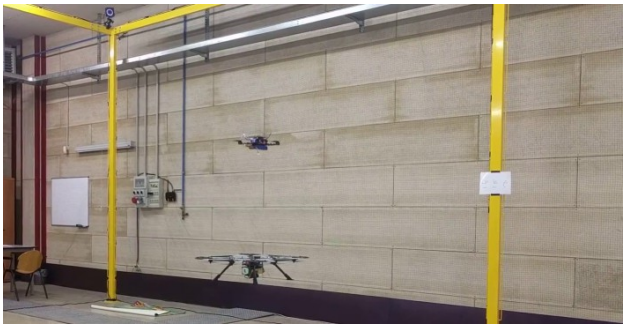

Fig. 4 ANT-R landing on the CARRIER-1 inside the FlyART facility

Particularly, the adopted UAVs are:

- Follower: a racer UAV, codename *ANT-R*, weighing 0.73 kg;
- Target: a octocopter, codename *CARRIER-1*, with a high thrust-to-weight ratio and a custom landing platform to ease the landing of the followers, weighing 2.9 kg;

The flight control system of both multirotors is divided into two hierarchical segments: a Flight Control Unit (FCU) which integrates the main Guidance, Navigation and Control features (GNC) and a Flight Companion Computer (FCC) which expands the UAV functionalities as the network communication. The FCU as low-level computer is based on an embedded system (STM32) and runs a Real-Time Operating System (RTOS) called NuttX, while the GNC features are performed by the *PX4 Autopilot* flight stack. As for the FCC, the adopted operating system, Raspbian, is a Linux distribution tailored for the embedded computers based on the Debian Operating System. The FCC is connected to a dedicated Wi-Fi network and

the communications with other UAVs or the Ground Control Station (GCS) are allowed by the Robot Operating System (ROS) middleware. Furthermore, the GCS has two main functionalities: to provide the attitude and position measured by the motion capture system (at a frequency of 100 Hz) and to send the position and heading trajectories to the UAVs using dedicated MATLAB functionalities. In particular, the guidance law which controls the position of both UAVs and the non-linear time-optimal landing algorithms are implemented in a MATLAB code running on the GCS as a centralized control architecture with an integration rate of 100 Hz and a set-point rate of 50 Hz.

7 Experimental results

The adopted benchmark which has been implemented to evaluate the landing performance of both guidance laws consisted firstly in a positioning of the two drones one above the other with a vertical relative distance $z_r^o(t_0) = 1.5\,\text{m}$ and then the execution of the landing trajectory. The telemetry data logged during the landing manoeuvres are reported in Figure 5 to 10. In Table 1 are reported the maximum acceleration and velocity bounds set as control parameters for both the guidance laws while in Table 2 are reported the obtained performance.

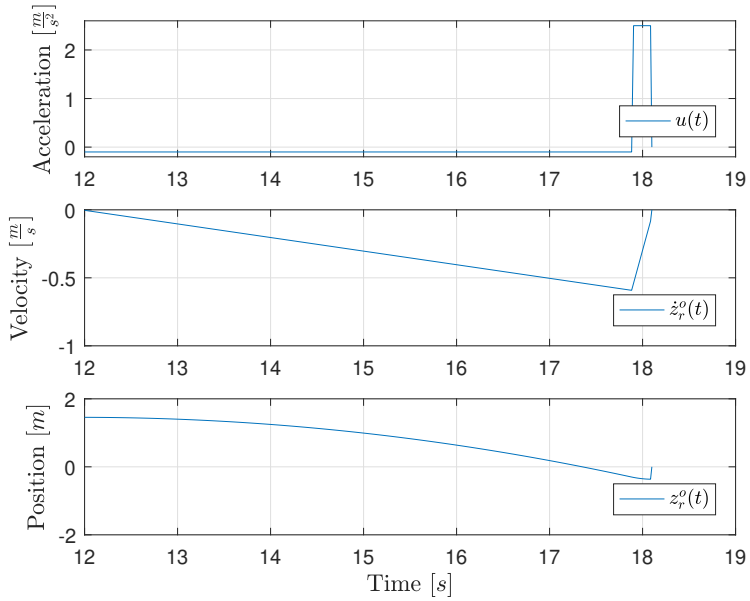

Fig. 5 *Bang-bang*: relative acceleration, velocity and position set-points

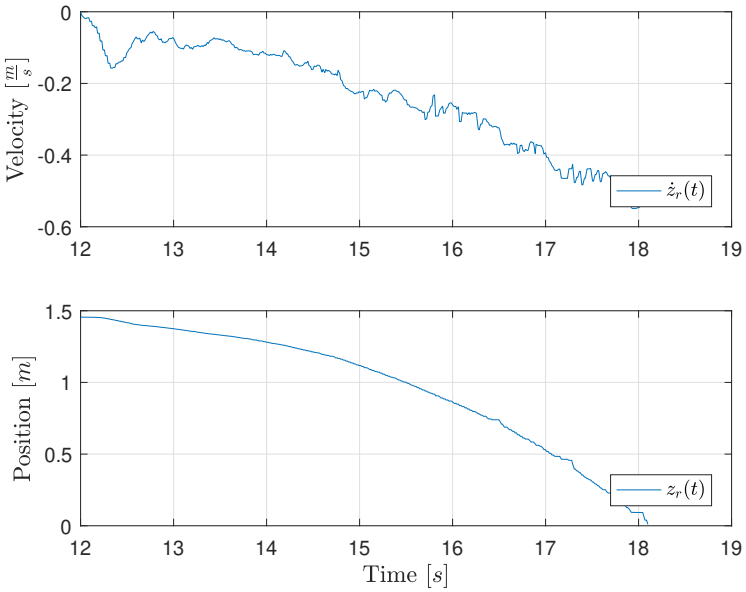

Fig. 6 *Bang-bang*: relative velocity and position

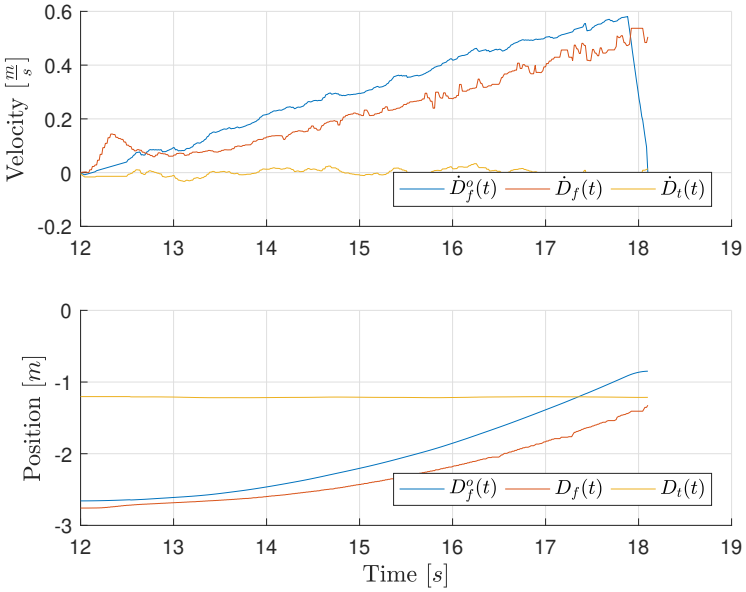

Fig. 7 *Bang-bang*: velocity and position set-points

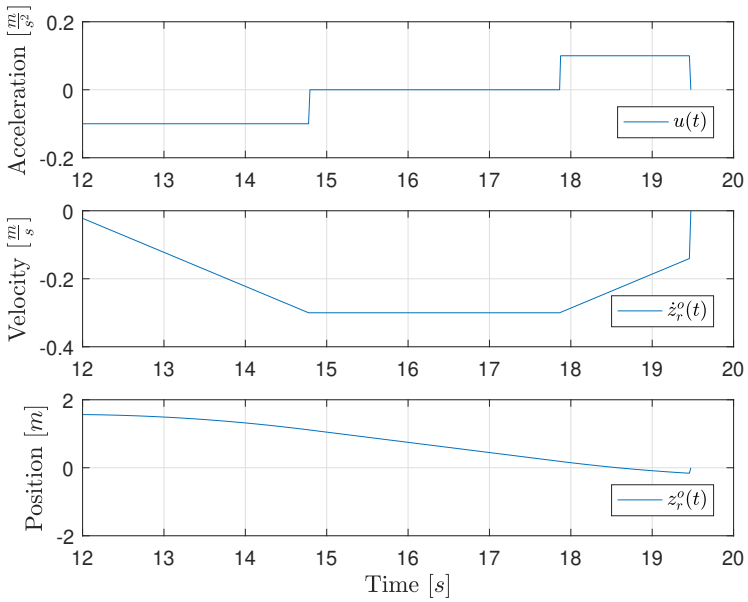

Fig. 8 *Bang-zero-bang*: relative acceleration, velocity and position set-points

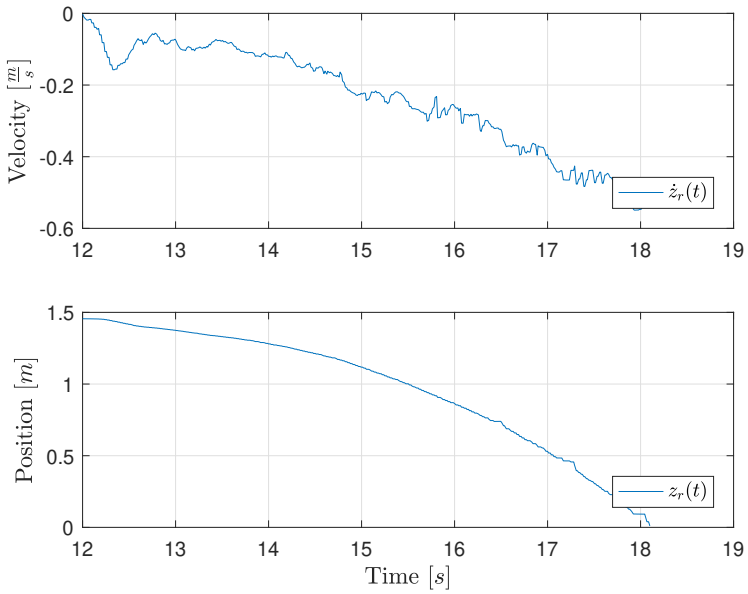

Fig. 9 *Bang-zero-bang*: relative velocity and position

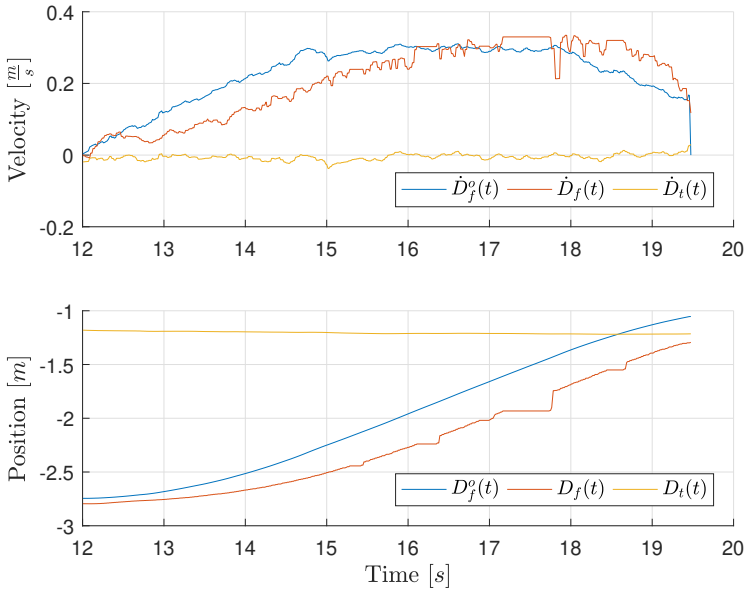

Fig. 10 *Bang-zero-bang*: velocity and position set-points

	bang-bang	*bang-zero-bang*
$\ddot{D}_f^{dec}$	$-2.5\,\mathrm{m/s^2}$	$-0.1\,\mathrm{m/s^2}$
$\ddot{D}_f^{acc}$	$0.1\,\mathrm{m/s^2}$	$0.1\,\mathrm{m/s^2}$
$\dot{D}_{max}^o$	-	$0.3\,\mathrm{m/s}$

Table 1 Control parameters

	bang-bang	*bang-zero-bang*
$t_l - t_0$	$6.1\,\mathrm{s}$	$7.5\,\mathrm{s}$
$\dot{z}_r(t_l)$	$-0.49\,\mathrm{m/s}$	$-0.088\,\mathrm{m/s}$

Table 2 Obtained performance

It is possible to observe that on one hand the *bang-bang* guidance law allows a faster landing but with a high touch-down speed, while on the other hand the *bang-zero-bang* guidance law, achieves a slower landing speed even though the landing requires more time.

8 Conclusions

In this paper, the problem of designing a nonlinear time-optimal guidance law for the air-to-air landing of a small quadcopter on a bigger octocopter has been studied and validated through experimental activities.

Given the obtained results, it is possible to conclude that the landing has been successfully performed for both the *bang-bang* and the *bang-zero-bang* case, although the first one demonstrated a less reliable performance. In general, the velocity and position tracking has not been accurate and this problem is caused by the position control architecture since such control loop is designed mainly for stabilization purposes and not for trajectory tracking. Nonetheless, the obtained results are satisfactory and they show the feasibility of this maneuver, opening a new research field of interactions between UAVs. Future work will include the redesign of the position control system, with a dedicated approach for trajectory tracking, the study of the horizontal motion and synchronization between the UAVs and the introduction of different UAV architectures (*i.e.*, fixed-wing carrier and multirotor lander).

References

1. T. Paul, T. R. Krogstad, and J. T. Gravdahl. Modelling of UAV formation flight using 3d potential field. *Simulation Modelling Practice and Theory*, 16(9):1453–1462, oct 2008.
2. F. Borrelli, T. Keviczky, and G. J. Balas. Collision-free UAV formation flight using decentralized optimization and invariant sets. In *2004 43rd IEEE Conference on Decision and Control (CDC) (IEEE Cat. No.04CH37601)*. IEEE, 2004.
3. Z. Chao, S. L. Zhou, L. Ming, and W. G. Zhang. UAV formation flight based on nonlinear model predictive control. *Mathematical Problems in Engineering*, 2012:1–15, 2012.
4. P. R. Thomas, U. Bhandari, S. Bullock, T. S. Richardson, and J. L. du Bois. Advances in air to air refuelling. *Progress in Aerospace Sciences*, 71:14–35, nov 2014.
5. C. Martinez, T. Richardson, and P. Campoy. Towards autonomous air-to-air refuelling for UAVs using visual information. In *2013 IEEE International Conference on Robotics and Automation*. IEEE, may 2013.
6. J. Valasek, K. Gunnam, J.r Kimmett, J. L. Junkins, D. Hughes, and M. D. Tandale. Vision-based sensor and navigation system for autonomous air refueling. *Journal of Guidance, Control, and Dynamics*, 28(5):979–989, sep 2005.
7. B. Herissé, T. Hamel, R. Mahony, and F. X. Russotto. Landing a VTOL unmanned aerial vehicle on a moving platform using optical flow. *IEEE Transactions on Robotics*, 28(1):77–89, feb 2012.
8. D. Lee, T. Ryan, and H. J. Kim. Autonomous landing of a VTOL UAV on a moving platform using image-based visual servoing. In *2012 IEEE International Conference on Robotics and Automation*. IEEE, may 2012.
9. J. W. Kim, Y. Jung, D. Lee, and D. H. Shim. Outdoor autonomous landing on a moving platform for quadrotors using an omnidirectional camera. In *2014 International Conference on Unmanned Aircraft Systems (ICUAS)*. IEEE, may 2014.
10. P. Vlantis, P. Marantos, C. P. Bechlioulis, and K. J. Kyriakopoulos. Quadrotor landing on an inclined platform of a moving ground vehicle. In *2015 IEEE International Conference on Robotics and Automation (ICRA)*. IEEE, may 2015.
11. B. Hu, L. Lu, and S. Mishra. Fast, safe and precise landing of a quadrotor on an oscillating platform. In *2015 American Control Conference (ACC)*. IEEE, jul 2015.
12. B. Chachuat. Nonlinear and dynamic optimization: from theory to practice. 2007. Url: http://lawww.epfl.ch/page4234.html.